




Investigation of the effect of offshore fixed wind turbine blades on fatigue damage of bases in the Hengam region in Iran

Yeganeh Jahandar ^a, Saleh Aminyavari ^{a,*}, Akbar Shahidzadeh Arabani ^a

Department of Civil Engineering, Chalous Branch, Islamic Azad University, Chalous, Iran

Article History: Received date 2022.04.08; revised date : 2022.05.24; accepted 2022.09.25

Abstract

Today, wind energy is considered as one of the most used types of renewable energy for electricity production. Over the past two decades, wind energy has been a major source of electricity, and electricity supply has been drastically increasing. Among the technologies available to generate electricity from wind, wind turbines play a major role, with offshore wind turbines playing a significant part. Offshore structures such as wind turbines, unlike other types of structures, are in a dynamic environment, the main forces generating this dynamic wave and wind environment, which impose significant structural vibrations, fatigue loads and significant loads on the blades, the turbine, structural platform, and other components import it. Welded joints and points in offshore structures are vulnerable to fatigue failure due to stress concentrations and intermittent environmental loading. Offshore structures have been exposed to shock forces and cyclic loads throughout their lifetimes, which cause the cyclic loads to cause fatigue in the joints. The dynamic forces of the waves gradually cause small cracks in the structural joints over time, and the expansion of these cracks at the weld foot and joints of the structural members reduces the overall stiffness of the joint and in some cases even removes the member from the location of connection. Much research has been done on the use of offshore wind energy, but despite the special attention of the worldwide scientific community on offshore wind energy extraction, there are still few studies domestically. Considering the water levels in the south of Iran and the platforms in the area will add to the importance of this study. The turbine structure will be examined to perform the research by using and inspiring DNV and API by-laws when the method is nonlinear. The case study will also cover the Strait of Hormuz and the time zone. This research is carried out using coding in Matlab as well as analysis in Bentley SACS finite element software which is dedicated to the design of offshore steel structures. The results indicate that the presence of the turbine blade geometry has a significant effect on the fatigue life of the retaining structure and the entire structure. (DOI:<https://doi.org/10.52547/JCER.4.2.1>)

Keywords: Blades, Offshore, Wind Turbines, Fatigue Damage, Hengam

* Corresponding author. Tel.: +989112912393; e-mail: saleh1161a@gmail.

1. Introduction

Over the past two decades, wind energy has received a great deal of attention as a source of electricity, and the supply of electricity using this source is increasing rapidly. Among the existing technologies for generating electricity from wind, wind turbines play the main role, among which offshore wind turbines play a significant part of this role, the attention to this part is increasing daily. Offshore structures such as wind turbines, unlike other types of structures, are in a dynamic environment, the main forces creating this dynamic environment are waves and winds, these forces, structural vibrations, fatigue loads and significant heavy loads to the blades. They import turbines, structural platforms, and other components. According to the mentioned conditions, today, the installation of offshore platforms in very deep waters and very unfavorable environmental conditions is also economically justified. Therefore, at present, extensive and increasing efforts are underway to provide solutions for the analysis and design of offshore structures against a variety of destructive phenomena, including the phenomenon of fatigue. Welded joints and joints in offshore structures are vulnerable to fatigue rupture due to stress concentrations and periodic environmental loading. One of the most important factors in immediate failure as well as reducing the strength of offshore platforms in the long run is the phenomenon of fatigue in the joints and structural members.

Wang et al. (2016) presented a stochastic dynamic response analysis for a 5MW vertical-axis floating wind turbine as a completely nonlinear coupling in the time domain. The FVAWT studied in this research, which is a combination of a Daris rotor and a semi-submersible float, is placed under different wind and wave conditions, and its overall motion, structural response, and elongation of inhibitory lines are simulated in the time domain as well as the domain. Frequency is obtained. In this research, the response of FVAWT in uniform and turbulent wind conditions is compared and the superiority of this type of turbine over the model with its fixed base in

reducing the effect of $2p$ on the dynamic response is shown [1].

Skaare et al. (2015) performed a comparative analysis between measurements made on the Hywind floating wind turbine main scale sample and its numerical simulations. In this study, they described the main characteristics of the Hywind structure, its control system and the important measurements made. In this research, a method for estimating the impact wave level to the Hywind structure is proposed and dynamic simulations comparable with the estimated time levels of the estimated wave level along with the measured statistical parameters of the wind field have been performed. Finally, the measured values of movement of roll, screw and yaw modes, tower bending torques, traction line tension, power generation, rotor speed and blade angle in both wind speeds lower and higher than the operating speed with simulations Numerical performed by SIMO / RIFLEX / HAWC2 numerical tool has been compared and has shown a very good fit [2]

Zhang et al. (2015) simulated the floating section and bracing system of a spar floating wind turbine with chain harness using Orcaflex software. In this research, by calculating the loads on the wind turbine, hydrodynamic analysis has been performed on the braking system and the tension of the braking lines under different loading conditions has been studied. Finally, using the obtained results, an optimal design for the desired inhibition lines was presented [3]

In 2016, Tamamgar et al. Feasibility study and location of offshore wind turbine fields on the shores of the Persian Gulf and the Sea of Oman, along with providing the optimal option of the basic turbine infrastructure and the optimal pattern of arrangement and arrangement of fields. In this study, after zoning, which is necessary to start a coherent research, wind information related to the southern regions of the country for 7 years, including the years 2000, 2005 and 2009 to 2013 were collected, and after classification and the creation of a data center Can be used for future work, annual averaging and determining the feasibility criteria of the regions according to the IEC standard, the study of the wind pattern of the region was performed to validate the information used. Also, at this stage of the research, it was found that there are compatible wind turbines on the mass production scale for the mentioned

region as well as regions with slightly lower speeds. In the next step, while introducing the types of fixed infrastructure used in the offshore wind industry and classifying their strengths and weaknesses, through a scoring system according to studies and considering the approximate depth of the potential area, which is approximately 50 meters, Jacket infrastructure was identified as suitable infrastructure [4]. Also, Baroni et al. (2016) Presented research entitled Dynamic Response Analysis of Offshore Floating Wind Turbines. In the present study, the motion responses for operating conditions have been investigated to evaluate the performance and structural stability of Spar floating wind turbine with chain restraint. To develop powerful design tools for the offshore wind industries, modeling requirements have been determined and the dominant physical processes have been calculated, and subsequently the BA-Simula model has been developed. Finally, the results obtained in the field of time and frequency are presented and using various validation methods, it is shown that the BA-Simula model simulates different loads well and can be a useful tool for estimating the physical behavior of the turbine. Floating wind turbines [5].

As the share of wind in the production of human energy is increasing, so are offshore wind turbine farms. An offshore wind turbine must be able to withstand the sea environment, which consists of wind and wave loads. The wind and wave create significant vibrations in the turbine structure and cause fatigue loads on the blade, the base of the structure and other turbine components. Fatigue loads increase maintenance operations, reduce turbine access, use expensive components, and ultimately break down turbine structures. Structure control technique can be used to reduce turbine vibrations and fatigue loads. So far, little scientific and laboratory research has been done in this field. Matthew et al. Investigated the passive control of offshore wind turbines and used mass dampers to control structural responses. A code called Fast is used to analyze the turbine. This is a program code written in the National Renewable Energy Laboratory. Also, for modeling the tuned mass damper (TMD), the Fast program was developed by Lackner and Rotea (2011) And is known as Fast-SC. In this research, a barge and monopile turbine have

been investigated. The results of this study show that the use of a TMD damper controls the turbine responses to incoming loads and thus reduces the turbine vibrations [6]

Hu and He (2017) Examined the semi-active control of floating base turbines. In this research, an adjustable fluid column damper has been used to control the turbine vibrations. In this research, infinite H algorithm is used to obtain feedback. The results of this study show that the application of liquid column dampers improves the performance of the turbine in the face of completely dynamic sea conditions and the vibrations of the structure are well controlled. [7].

Colwel and Basu (2009) Also investigated the structural control of offshore wind turbines using liquid column dampers. In this study, the turbine has been modeled as a multi-degree of freedom structure. The Kaimal and JONSWAP spectra have been used to model wind and wave load, respectively. The results of this study show that with the use of liquid column dampers, the maximum response of the structure is reduced by about 55%. This reduction in turbine structure vibrations reduces turbine construction costs. Also, increasing the damper amplitude increases the fatigue life of turbine components [8].

In research by Thompson and Sørensen (1999), an increase in fatigue load in the wind farm compared to free flow was found between 5 and 15% depending on the wind farm design. The increase in load because of awakening was the same for a marine and terrestrial site [9].

Hakmabadi et al., (2016) investigated the application of a tuned mass damper with different masses, in an offshore Tension Leg Platform (TLP). Tuned Mass Dampers (TMDs) modeled in a developed code FAST-SC. Results show that using TMD in the nacelle can reduce the moments in the base of the tower and turbine vibration. This reduction can also increase time until failure factor of the OWTs. [10].

2. Methodology

The information corresponding to the specifications of the wind turbine support structure

studied in this region is given in Table 1. It is worth mentioning that 5 class levels have been considered to investigate the phenomenon of fatigue in this study, of which 3 class levels are below the water level and 2 class levels are above the base level.

Table 1
Specifications of wind turbine holding structure studied in this area

Water depth at the place of installation of wind turbine structure	61.5 meters
Height of wind turbine jacket to the bottom of the sea	81 meters
Base of the structure	140 cm diameter, thickness 2.5 cm
Details of class levels	+9, +5.75, -6, -18-, -37.5
Angle of sea waves entering the structure of wind turbine holder	45° (8 directions)
specific gravity of water	$\rho=1025 \text{ kg/m}^3$

In this research, the material of the supporting structure and wind turbine will be strong steel. The specifications of the materials in the steel section of the structure will be as shown in Table 2.

Table 2
Characteristics of materials used in the case platform model

Special Weight (kN /cm ²)	yield stress (kN /cm ²)	Shear modulus (kN /cm ²)	modulus of elasticity (kN /cm ²)
7850	35.50	7921	20590

To apply the loading section to the wind turbine structure under study, information obtained from design companies as well as experts and specialists should be provided. Among these, data such as wind information from different geographical directions,

water depth and storm wave data, 1-year and 100-year wave information, and flow information are in the focus of considerable importance.

In the following, in Table 3, the information corresponding to the wind speed that occurred in the Hengam area in the 1-year operating conditions and the so-called 100-year emergency conditions are listed.

Table 3
Water depth, storm surge and wind speed in Hengam Region

Parameter	Depth (m)							
	SE	E	NE	N	NW	W	SW	S
LAT above seabed	61.5							
MHHW above LAT	1.6							
Storm surge (100 yrs)	0.3	0.2	0.1	0.1	0.3	0.2	0.1	0.2
Storm surge (1 year)	0.2	0.1	0.1	0.1	0.2	0.1	0.1	0.1
Total SWL (100 yrs)	63.4	63.3	63.2	63.2	63.4	63.3	63.2	63.3
Total SWL (1 year)	63.3	63.2	63.2	63.2	63.3	63.2	63.2	63.2
	Wind speed (m/s)							
	SE	E	NE	N	NW	W	SW	S
Wind speed (1 year)	21.7	22.2	21.5	27.6	22.7	22	20.4	20.6
Wind speed (100 yrs)	35.2	36	34.9	35.6	36.7	35.6	33	33.4

Water depth and storm wave data of the region When in the path of digitization and completion of depth data in the study area, the base level around the LAT level is 61.5 meters. This level is the lowest level of the astronomical tide from the seabed to the water level. Also, the value corresponding to MHHW (Mean Higher High Water) above the LAT level is 1.6 meters. Storm wave values as well as total water levels for 1-year operating conditions and so-called 100-year emergency conditions are also listed.

The wave information of the study area includes the characteristic wave height (in meters) and the wave period (in seconds) in the case of one-year and 100-year return periods in different directions of

application according to Table 4. As can be seen from the table, the minimum value of the characteristic wave height for a one-year return period is from the southwest direction by 5 meters and the maximum value is 6.7 meters from the northwest direction. The mentioned values correspond to the 100-year return period are 8.8 meters from the southwest and northeast and 12.2 meters from the northwest, respectively.

Table 4
1-year and 100-year wave information

Parameter	Wave (1 year)							
	SE	E	NE	N	NW	W	SW	S
Height (m)	6.3	6	5.1	5.5	6.7	6	5	5.6
Period (s)	8.3	8.1	7.5	7.8	8.6	8.1	7.4	7.9
	Wave (100 yrs)							
	SE	E	NE	N	NW	W	SW	S
Height (m)	11.6	10.8	8.8	9.7	12.2	10.8	8.8	10.2
Period (s)	10.8	10.4	9.6	10	11	10.4	9.5	10.2

Flow data Operational and extraordinary conditions for the Hengam area in both bed conditions are considered as rough and flatbed conditions in explaining the flow force. Also, 4 selected levels to provide a more tangible relationship with this phenomenon in the study environment are presented. These 4 levels include the current at the surface, the current at medium height, the current at a depth of 1 meter from the seabed and the current at a depth of 0.5 meters above the seabed. It is necessary to mention that to create a reliability coefficient in the design, the amount of flow velocity at the middle height is equal to the amount of flow at the surface. These values are given in Table 5 in full. The flow velocity in this research is considered in meters per second.

Table 5
Flow information

Flow condition	Flow velocity in rough bed	Flow velocity in flat bed
Surface flow	0.9	1.28
Flow in middle height	0.9	1.28
1 meter above the seabed	0.68	0.78
0.5 meter above the seabed	0.62	0.71

2.1. The Coefficient of Morrison equations

Wave force calculations are divided into two categories. In small platforms or platforms that are installed in relatively shallow water, the design related to the wave forces is done by loading static forces on the structure. In taller structures where the natural period of vibration of the structure is closer to the period of sea waves, a complex dynamic analysis must be performed. In this article, only static design is studied. Wave design forces should be considered based on the worst conditions caused by hurricanes with a return period of 111 years. In calculating the water depth in the storm mode, high storm waves with normal tides should be considered. The design wave for static analysis of waves is determined by the client whose structure is designed to his order. The horizontal force exerted by the waves on a cylindrical member consists of two parts, one is the drag force from the kinematic energy of water and the other is the inertial force from the acceleration of water particles. To obtain the total force on a member, the water pressure is multiplied by the volume or area of the member image perpendicular to the direction of the wave current. This force is calculated along the member unit using the relation provided by Morison, O'Brien, Johnson, and Schaaf, 1950. This relationship of force on a pipe result in two components, inertia, and drag. This relationship is as follows:

$$F = F_I + F_D \quad (1)$$

$$F = C_m \frac{w\pi D^2}{g} \frac{du}{dt} + C_d \frac{1}{2} \frac{w}{g} Du|u|$$

The values of cm and cd are obtained through experiments and modeling, depending on the shape and size of the tube, the amount of mass added to it in water, and the type of wave theory used to calculate the velocity and acceleration of water particles has it. In this study, the drag and inertia coefficients cm and cd in Morison relation are considered according to Table 6. These coefficients will be dimensionless.

Table 6
Drag and inertia coefficients

Members	C_{dN}	C_{mN}
Flat tube members	1.6	1.6
Smooth tube members	0.65	1.6
Coarse tube members	1.05	1.20

2.2. Effect of growth on the surface of the structure

Due to the difference in thickness created by the growth of seaweed on the cross section of the offshore wind turbine body structure and its effect on the coefficients and values of the Morrison equation, this parameter will be one of the components affecting the research results. This item is considered in two parts. Thus, from the class level of +2 to the class level of -6, a section and from the class level of -6 to the mudline are considered as the second section. The amount of thickness added to different parts of the wind turbine base is according to Table 7.

Table 7
Amount of thickness added to different parts of the wind turbine

Thickness	Elevation	Dry density
Radius 75 mm	+2 to -6	1400 kg/m ³
Radius 75 mm decreasing to 50 mm	-6 to mudline	

2.3. Modeling of wind turbine implementation

Analysis of wind turbine structure using three-dimensional model includes support structure and deck, outer cylinder of wind turbine and wind turbine blades. Accessories such as shock absorbers and floating landings are also installed to calculate the peripheral loads. The structure under study is explained in the part of the support body and the deck of the turbine. Information about situations such as the introduction of middle floor levels, level change angle of structural foundations, bed level, pile, and

deck connection section, piling specifications of the structure are provided in this section.

In the following, the specifications of the wind turbine structure foundations are mentioned in terms of the number and rows of calls to the software, the slope of the foundations and the state of pile and base interference. It is worth mentioning that the supporting structure will be considered as 3 bases. In the next stage of design, the dimensions of structural sections, structural joints and details of loading sections will be considered. In the following and in Figure 1, the wind load loading conditions are given in the selected direction of zero degrees with a velocity of 27.6 meters per second. The three-dimensional schematic shown in the figure shows the details of the offshore wind turbine support structure in sections such as the work point, Fender.

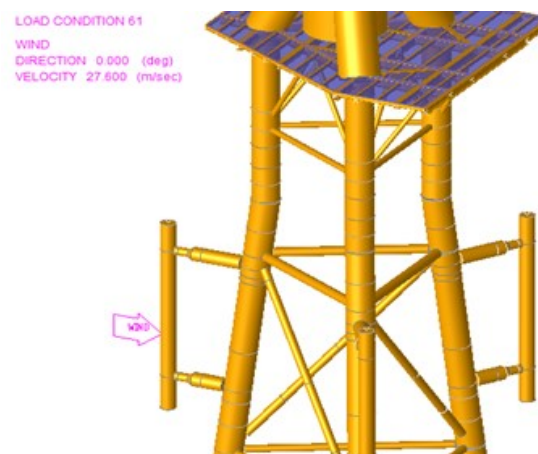


Figure. 1. Applying wind force to the structure

According to Figure 2 simultaneously, the profile corresponding to the application of wave force and current on the structure is presented.

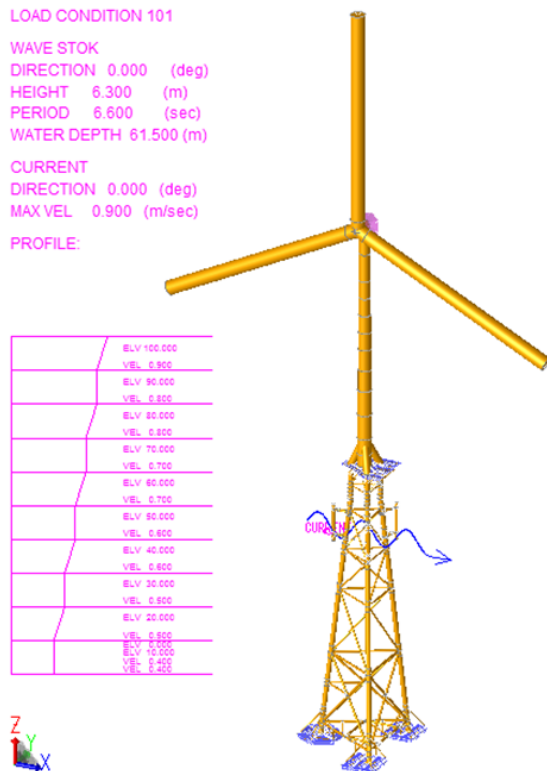


Figure. 2. Simultaneous application of wave force and current on the structure

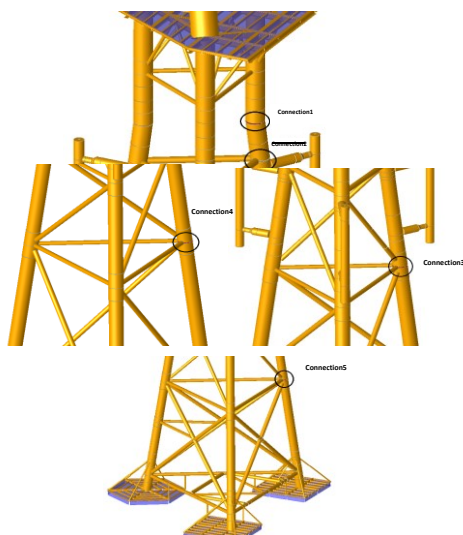


Figure. 3. Connection1 at level -6 meters above water level and connection2 at level +5.8 meters, Connection3 at level +9 meters above water level, connection4 at level -18 meters and connection5 at level -37 meters relative to water level

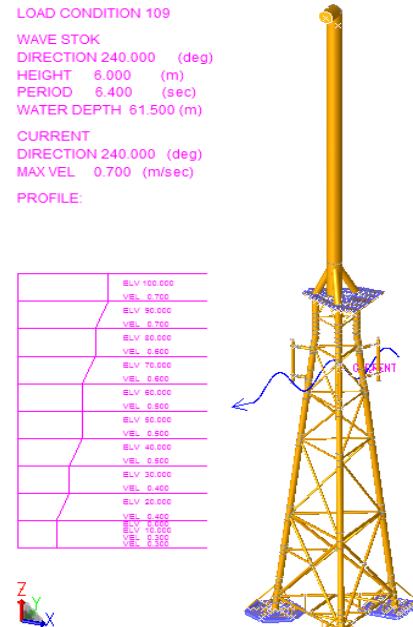


Figure. 4. Simultaneous application of wave force and current on a bladeless structure

2.4. Fatigue analysis method used in the research

As mentioned, to calculate the fatigue damage inside the structure, several methods can be calculated. In this research, we use the Determinant method. Determinant analysis is in fact static in nature and the dynamic properties of the structure are considered in a dynamic incremental coefficient.

In the first stage, by solving the wave equation, the velocity and acceleration of the particles are stored as a function of the depth and angle of the wave phase in a matrix so that these data can be used in the next step.

In the second stage, the geometry and dimensions of the structure are received as input and using the Morrison equation, the wave force is applied as a wide load on the structure and the wave load is converted to knot forces. At this stage, the wave

phase angle is changed from zero to 360 degrees and in each phase angle, according to the position of the relevant element relative to a base point (zero coordinates of the structure), the wave force is converted to nodal forces in structural analysis. To be used.

At the end of the second stage, the wave force in all members is converted to nodal loads and used in the matrix of stored nodal forces in structural analysis.

In the third stage, first, by performing an analysis of special values in the structure, the periodicity of the structure is used and according to the periodicity of the wave and the structure, the Dynamic Amplification Coefficient (DAF) will be calculated.

$$DAF = \frac{1}{\sqrt{[1 - (\frac{TS}{TW})^2]^2 + [2\xi(\frac{TS}{TW})]^2}} \quad (2)$$

Table 8

Natural Periods of Jacket Platform

MODE	FREQ.(CPS)	GEN. MASS	EIGENVALUE	PERIOD(SECS)
1	0.408745	2.7393324E+03	1.5161241E-01	2.4465115
2	0.619758	2.0726531E+03	6.5947035E-02	1.6135318
3	0.622837	1.6413069E+03	6.5296797E-02	1.6055573
4	2.129900	1.7763440E+03	5.5836977E-03	0.4695057
5	2.195281	1.4941853E+03	5.2560553E-03	0.4555225
6	2.866091	2.4158849E+03	3.0836153E-03	0.3489072
7	2.944449	3.9777338E+02	2.9216777E-03	0.3396222
8	3.007557	4.7962469E+01	2.8003514E-03	0.3324958
9	3.327140	2.8971882E+01	2.2882213E-03	0.3005584
10	3.431388	2.1694043E+03	2.1512974E-03	0.2914272

Table 9

The force and moment on the structure of the first state jacket with vertical bases

BASE SHEAR AND OVERTURNING MOMENT COEFFICIENTS				
MODE	SHEAR(X) KN	SHEAR(Y) KN	MOMENT(X) KN-M	MOMENT(Y) KN-M
1	-1351.462	-1.772	-34.303	15597.192
2	1.779	-1864.761	-24285.719	-7.030
3	9.535	-35.679	4556.879	-1478.847
4	4.618	-4260.251	-448642.306	-207.627
5	-4979.900	-1.925	-195.807	476287.867
6	-105.461	-190.077	-11200.575	10048.278
7	-2003.320	-64.148	-4014.283	-11837.978
8	-169.663	1390.891	83878.865	19560.346
9	-11.175	-6780.121	-336782.681	3538.965
10	-5850.145	47.073	5050.972	162775.367

We considered the structural modes to be ten, the first three modes being the most important mode, and the period of the structure with angle-free bases being 2.446 seconds, which is in accordance with the standard API regulations and less than three seconds. Which is mentioned in the regulations for the Persian Gulf region.

In the fourth stage, using the matrix of node forces obtained from the second stage and the dynamic amplification coefficient obtained from the third stage, structural analysis is performed in the structure using SACS software [11] and the forces in the members leading to the connection will be stored at all angles of the wave phase.

In the fifth stage, according to the connection geometry and members, the stress coefficients in each connection are obtained and by using the forces obtained from the fourth stage, the stress in the inflamed area in all the restraints of the connection on both sides of the restraint and the main member will be obtained. In each connection, the maximum and minimum stress will be selected from all angles of the wave phase by maintaining its algebraic sign, and by using these two values, changes in the stress interval in each connection will be obtained.

In the sixth step, according to the values of stress efficiency obtained in each joint using the stress-life curve, the maximum number of tolerable cycles within the joint is determined and according to the number of load cycles in the structure and according to Palmgren-Miner Rule [12], fatigue damage accumulation in the structure will be calculated. The wave scatter diagram in the fatigue life evaluation is shown in the table below.

Table 10

Magnification coefficient correction for 1-year and 100-years

Wave direction	1-year	DAF 1-year	100-years	DAF 100-years
West	8.1	1.0426	10.4	1.023
Southwest	7.4	1.0514	9.5	1.03
South	7.9	1.0448	10.2	1.026
Southeast	8.3	1.040	10.8	1.023
East	8.1	1.0425	10.4	1.025
Northeast	7.5	1.05	9.6	1.029
North	7.8	1.046	10	1.027
Northwest	8.6	1.037	11	1.022

The desired life of the design, which is recommended in the API regulations for the life of the jacket platform bases based on 50 years, must be defined. In the theory of irregular waves, there are various spectrums that used the Pearson Moskvich spectrum.

To establish a more tangible relationship with the current phenomenon under study, in Figure 5, the current force profile on the platform is drawn. The values of flow velocity are not zero at the bed level and have a value of 0.69 m/s, and as we get closer to the surface, this value increases and changes in a parabolic manner.

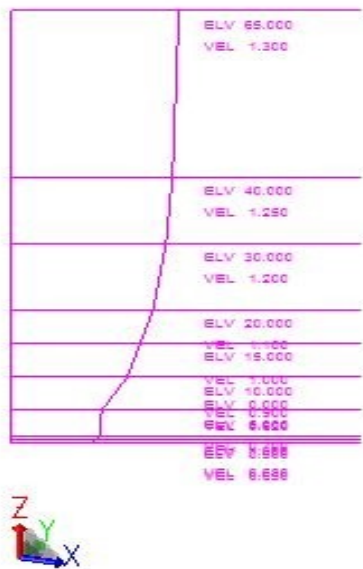


Figure. 5. Profile of the current force acting on the platform

As previously mentioned, the platform studied in this research is a 4-base jacket platform and the order of numbering the platform bases is as follows.

It is worth mentioning that base-1 and 2 - 3 and 4 are of the same type and the characteristics of the material and the base angle (1 and 2), (3 and 4) each are equal. In this issue, due to the large volume of results and the duration of finite element software in this research, we examine the first and third bases. Base number two has the same results as base number one and base number four has the same results as base three. In the following, we considered four connections in the level of each floor. We

considered the location of these connections as the connection of the class level to the base of the platform (joint) as shown in Figure 6. The reason for choosing this place is that punching is done in this area, and it is one of the most critical connections.

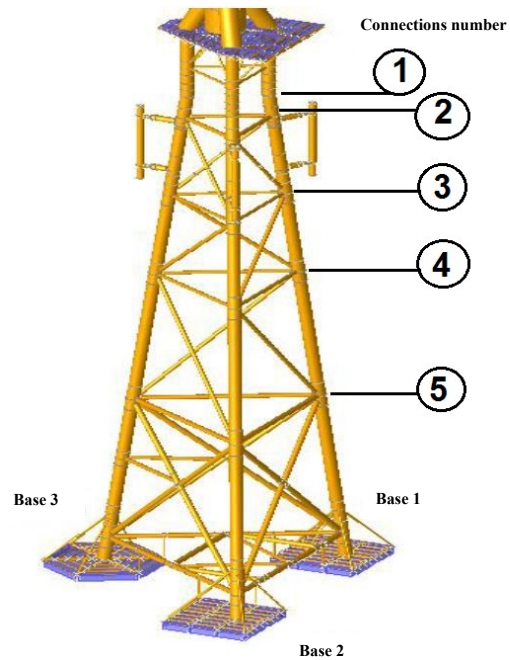


Figure. 6. Numbering the bases of the wind turbine holding structure

3. Result

After performing several analyzes on both output modes, the fatigue damage is attached to the following.

Table 11

Calculation of fatigue damage in four base connections 1 and 2 in platform mode with pile-soil interaction

*** HENNER FATIGUE REPORT ***														
(JOINT ORDER)														
JOINT	MEMBER	GRUP	TYPE	ORIGINAL	CHORD								FATIGUE RESULTS	
ID	ID		ID	OD (CH)	WT (CH)	JNT TYP	MEM TYP	LEN. (H)	GAP (CH)	STRESS AX-CR	CONC. AX-SD	FACTORS IN-PL	DAMAGE LOC	SUC LIFE
1041	1041-0000	CLQ	TUB	170.00	5.00	Y	BRC	25.28		2.00	2.00	2.00	2.00	1.095679 L 68.45870
1031	1031-3430	CLH	TUB	170.00	5.00	Y	BRC	28.55		2.00	2.00	2.00	2.00	.9592742 TR 78.18410
1021	1021-2020	CLQ	TUB	170.00	5.00	Y	BRC	25.28		2.00	2.00	2.00	2.00	.9912464 R 75.46232
1011	1011-0005	CL	TUB	170.00	5.00	T	BRC	28.41		2.00	2.00	2.00	2.00	.6910005 B 100.5383

Table 12

Calculation of fatigue damage in four base connection1 in platform mode without pile-soil interaction (seabed rigidity)

* * * MEMBER FATIGUE REPORT * * *													
(JOINT ORDER)													
JOINT	MEMBER	GROUP	TYPE	ORIGINAL	CHORD	GAP * STRESS CONC. FACTORS *				FATIGUE RESULTS			
ID	ID			DO (CH)	VT (CH)	JNT TYP	LEN. (H)	AS-CH	AS-SD	IN-PL	OU-PL	DAMAGE	LOC SUC LIFE
1041	1041-3408	CLH	TUB	178.00	5.00	Y	20.55	2.00	2.00	2.00	2.00	1.828778	L 73.47396
1031	1031-3408	CLH	TUB	178.00	5.00	Y	20.55	2.00	2.00	2.00	2.00	.9616520	TR 77.99879
1021	1021-2828	CLQ	TUB	178.00	5.00	Y	25.28	2.00	2.00	2.00	2.00	.4728388	L 158.6164
1011	1011-0885	CL	TUB	178.00	5.00	T	28.41	2.00	2.00	2.00	2.00	.4482801	B 178.3759

Table 13

Calculation of fatigue damage in four base connection1 in platform mode without pile-soil interaction (seabed rigidity)

* * * MEMBER FATIGUE REPORT * * *													
(JOINT ORDER)													
JOINT	MEMBER	GROUP	TYPE	ORIGINAL	CHORD	GAP * STRESS CONC. FACTORS *				FATIGUE RESULTS			
ID	ID			DO (CH)	VT (CH)	JNT TYP	LEN. (H)	AS-CH	AS-SD	IN-PL	OU-PL	DAMAGE	LOC SUC LIFE
3041	3041-0810	CLH	TUB	178.00	5.00	Y	18.94	2.00	2.00	2.00	2.00	1.287619	B 61.99596
3031	3031-3468	CLH	TUB	178.00	5.00	Y	20.55	2.00	2.00	2.00	2.00	.9621229	TR 77.95262
3021	3021-2638	CLQ	TUB	178.00	5.00	Y	25.28	2.00	2.00	2.00	2.00	.9999638	R 75.88278
3011	3011-0975	CL	TUB	178.00	5.00	T	28.41	2.00	2.00	2.00	2.00	.8033468	B 93.35943

Table 14

Calculation of fatigue damage in four connections of base3 in platform mode without pile-soil interaction (seabed rigidity))

* * * MEMBER FATIGUE REPORT * * *													
(JOINT ORDER)													
JOINT	MEMBER	GROUP	TYPE	ORIGINAL	CHORD	GAP * STRESS CONC. FACTORS *				FATIGUE RESULTS			
ID	ID			DO (CH)	VT (CH)	JNT TYP	LEN. (H)	AS-CH	AS-SD	IN-PL	OU-PL	DAMAGE	LOC SUC LIFE
3041	3041-0828	CLH	TUB	178.00	5.00	Y	20.55	2.00	2.00	2.00	2.00	1.289756	TR 62.18569
3031	3031-0828	CLH	TUB	178.00	5.00	Y	20.55	2.00	2.00	2.00	2.00	.9683837	TR 78.89379
3021	3021-0828	CLQ	TUB	178.00	5.00	Y	25.28	2.00	2.00	2.00	2.00	.5445189	L 137.7363
3011	3011-0828	CL	TUB	178.00	5.00	T	28.41	2.00	2.00	2.00	2.00	.5869366	B 147.9475

3.1. Validation of output results

At the end of the research, to validate the research and in fulfilling the validation item, the amount of fatigue life obtained in the connections of the jacket platform bases will be examined and compared with the valid API regulations [13]. The paragraph used is as shown in Figure 7.

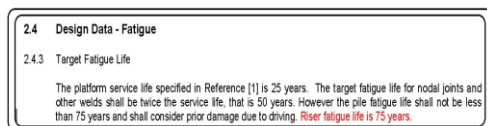


Figure. 7. Paragraph used in the API regulations

Figure 8 shows that the results are acceptable for the fatigue design life of the platform joints (50 years).

4. Conclusion

In this research, a structure with the use of non-fossil and natural wind energy extraction is made of four separate structures, which include the deck of the structure in the form of a cylinder and wind turbine as the main part of the research, retaining structure and piles buried in the seabed. Usually, most of such research have omitted the presence of the candle section and have considered the seabed rigidly, but in this dissertation, the existence of a candle has also been considered and the seabed has been considered as elastic.

Considering the interaction of piles, soil and supporting structures with wind turbines and cylinders connected to it for some analyzes including fatigue analysis, earthquake analysis, static structure analysis, dynamic structure analysis, ship impact analysis and even important material analysis will be.

After one of the wind turbine structures in Hengam area located in the Strait of Hormuz and the southern part of Qeshm Island, was considered, the fatigue analysis of the body of this wind turbine structure with the presence of piles and soil was done

by time history method and main outputs Achieved and attached.

The minimum fatigue life designed for the bases of wind turbine structures in the API regulations is based on 50 years, the service life for the first and second base in four class levels is a maximum of 108 years and a minimum of 68 years, and life Service for grades three and four in four class levels is a maximum of 93 years and a minimum of 62 years.

As can be seen, the closer we get to the seabed level, the less wave and current force and the longer the service life at lower levels, and vice versa, the closer we get to the water level, the higher the wave and current force reached, and the service life is reduced. This issue is briefly at the wave and current profiles and the collision with the structure is completely transparent, which is mentioned in most marine structural engineering references.

As can be seen, the minimum design life of wind turbine structure foundations is longer than the life recommended in the regulations.

In explaining the fatigue phenomenon of offshore structures such as wind turbines and fixed platforms, the time history method is more accurate than the definite method, because, in the time history method, the structure is studied hydrodynamically, but in the definite method in static form. As a result, the results of time history analysis outputs are closer to reality.

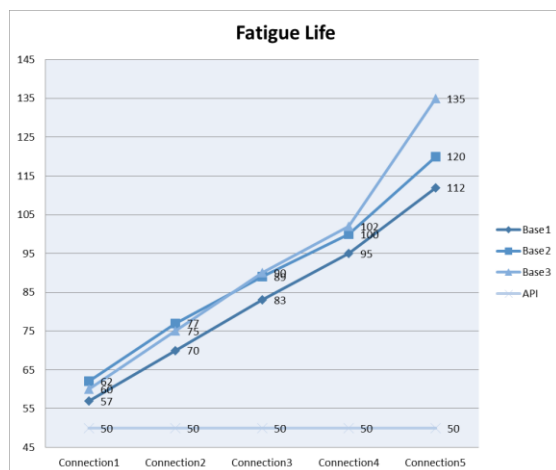


Figure.8 Validation of model results

References

- [1] Wang, K., Moan, T., & Hansen, M. O. (2016). Stochastic dynamic response analysis of a floating vertical-axis wind turbine with a semi-submersible floater. *Wind Energy*, 19(10), 1853-1870.
- [2] Skaare, B., Nielsen, F. G., Hanson, T. D., Yttervik, R., Havmøller, O., & Rekdal, A. (2015). Analysis of measurements and simulations from the Hywind Demo floating wind turbine. *Wind Energy*, 18(6), 1105-1122.
- [3] Zhang, D. P., Zhu, K. Q., Jing, B., Yang, R. Z., & Tang, Z. C. (2015). Dynamic analysis of the mooring system for a floating offshore wind turbine spar platform. *International Conference on Computer Information System AND industrial Applications*, 3(3.5), 1.
- [4] Tamamgar A., Adjami M., Kazemi Nezhad M.H., (2016). Feasibility study on offshore wind farms in Persian Gulf and Oman Sea, and proposing optimal substructure and layout for assumed wind turbines and wind farms in the studied area. *Master Thesis in Khorramshahr University of Marine Sciences and Technology*.
- [5] Baroni M., Alali N., Bakhtiari M., Sadrinasab M (2016). Dynamic Response Analysis of Offshore Floating Wind Turbines. *Master Thesis in Shahrood University*.
- [6] Lackner, M. A., & Rotea, M. A. (2011). Structural control of floating wind turbines. *Mechatronics*, 21(4), 704-719.
- [7] Hu, Y., & He, E. (2017). Active structural control of a floating wind turbine with a stroke-limited hybrid mass damper. *Journal of Sound and Vibration*, 410, 447-472.
- [8] Colwell, S., & Basu, B. (2009). Tuned liquid column dampers in offshore wind turbines for structural control. *Engineering structures*, 31(2), 358-368.
- [9] Hokmabady, H., Mojtahedi, A., & Lotfollahi Yaghin, M. A. (2016). Structural Control and Fatigue Analysis of Offshore TLP Wind Turbine Using TMD. *Journal Of Marine Engineering*, 11(22), 39-50.
- [10] SACS manual, Fatigue, Release 6.
- [11] Zhao, X. L., Wilkinson, T. J., & Hancock, G. (2005). *Cold-formed tubular members and connections: Structural behaviour and design*. Elsevier.
- [12] American Petroleum Institute. Recommended Practice for Planning, Designing and Constructing Fixed Offshore Platforms-Working Stress Design, Twenty first edition, December 2000.